

# The Effect of Transition Metal Additions (Mo and W) on Double Oxide Film Defects in an Al-Si-Mg Alloy

Griffiths, William; Caden, A.J.; Chen, Qi

DOI:

[10.1080/02670836.2017.1346911](https://doi.org/10.1080/02670836.2017.1346911)

License:

Other (please specify with Rights Statement)

*Document Version*

Peer reviewed version

*Citation for published version (Harvard):*

Griffiths, W, Caden, AJ & Chen, Q 2017, 'The Effect of Transition Metal Additions (Mo and W) on Double Oxide Film Defects in an Al-Si-Mg Alloy', *Materials Science and Technology*.  
<https://doi.org/10.1080/02670836.2017.1346911>

[Link to publication on Research at Birmingham portal](#)

## **Publisher Rights Statement:**

This is an Accepted Manuscript of an article published by Taylor & Francis in Materials Science and Technology on 12th July 2017, available online: <http://www.tandfonline.com/10.1080/02670836.2017.1346911>

## **General rights**

Unless a licence is specified above, all rights (including copyright and moral rights) in this document are retained by the authors and/or the copyright holders. The express permission of the copyright holder must be obtained for any use of this material other than for purposes permitted by law.

- Users may freely distribute the URL that is used to identify this publication.
- Users may download and/or print one copy of the publication from the University of Birmingham research portal for the purpose of private study or non-commercial research.
- User may use extracts from the document in line with the concept of 'fair dealing' under the Copyright, Designs and Patents Act 1988 (?)
- Users may not further distribute the material nor use it for the purposes of commercial gain.

Where a licence is displayed above, please note the terms and conditions of the licence govern your use of this document.

When citing, please reference the published version.

## **Take down policy**

While the University of Birmingham exercises care and attention in making items available there are rare occasions when an item has been uploaded in error or has been deemed to be commercially or otherwise sensitive.

If you believe that this is the case for this document, please contact [UBIRA@lists.bham.ac.uk](mailto:UBIRA@lists.bham.ac.uk) providing details and we will remove access to the work immediately and investigate.

# **The Effect of Transition Metal Additions (Mo and W) on the Behaviour of Double Oxide Film Defects in an Al-Si-Mg Alloy**

W. D. Griffiths, A. J. Caden and Q. Chen.

School of Metallurgy and Materials,

College of Engineering and Physical Sciences,

University of Birmingham, Edgbaston, Birmingham,

United Kingdom. B15 2TT.

**Corresponding author: W. D. Griffiths**

**Email:** [W.D.Griffiths@bham.ac.uk](mailto:W.D.Griffiths@bham.ac.uk)

**Tel.:** 0121 414 5246

**Fax.:** 0121 414 5232

**Word Count:** 4327 (excl. references)

**Keywords:** Al alloys, casting, defects, oxide films, Weibull Modulus, molybdenum, tungsten, tensile properties.

## **Biographies**

Dr. W D Griffiths received his PhD from Sheffield City Polytechnic, and then became Senior Research Associate at the University of Nottingham, investigating electromagnetic stirring in Al alloys. This was followed by the position of Federal-Mogul Research Fellow at UMIST, to carry out research into interfacial heat transfer during casting solidification. He is currently Senior Lecturer at the School of Metallurgy and Materials, University of Birmingham, where his research interests involve the study of heat transfer and fluid flow during the casting of light alloys, Lost Foam casting of Al alloys, and the development of techniques using radioactive particle tracking in liquid metals. Mr. A J Caden is manager of the Castings Laboratory at the University of Birmingham. Dr. Qi Chen received his BSc degree from Central South University in China, majoring in Materials Science and Engineering, and was a PhD student at the School of Metallurgy and Materials, University of Birmingham, when this work was carried out.

## **ABSTRACT**

Double oxide film defects in Al alloys have been associated with reduced mechanical properties and increased variability in properties in cast Al alloys. This paper explores the effects of the addition to an Al-7Si-0.3Mg alloy (2L99) of around 0.4 to 0.5wt.% of the transition metals Mo or W. The variability of tensile properties was significantly reduced, resulting in an approximate doubling of the values of the Weibull Modulus of the Ultimate Tensile Strength, and an increase of 10 to 20% in the Weibull Modulus of the %Elongation. Scanning Electron Microscopy EM examination of the fracture surfaces revealed the presence of oxide films, as expected, but also found AlN. The mechanism(s) by which Mo or W additions improve mechanical properties has not been established but the presence of AlN suggested the accelerated consumption of the internal atmosphere of the double oxide film defects, leading to a reduction in their size and hence their deleterious effects.

## 1. Introduction.

To better exploit Al alloys the effect of defects on mechanical properties requires greater study. Since the publication of Campbells' review of the casting process in 1992, now into its fourth edition [1], the light alloy casting community has become increasingly aware of the impact of double oxide film defects on the properties of Al alloys, (also known as "bifilms"). These occur due to the entrainment of the oxidised surface skin of the liquid Al. This surface oxide film can easily rupture but would reform virtually instantaneously, due to the high reactivity of Al with oxygen in the atmosphere. A continuous oxide film can therefore be assumed to be constantly present on the surface of the liquid metal. When the liquid metal is transferred in some way as part of the melting and casting operation, such as being poured into a mould, it can form a splash that then recombines with the bulk liquid. This carries into the melt the folded-over oxidised surface of the liquid metal, together with a small gas pocket. This probably contains the local atmosphere, perhaps consisting largely of air, (shown schematically in Figure 1). It has been reasoned that the presence of the oxide film on the internal surfaces of the doubled-over film would prevent the sides of the defect from bonding together, partly because sintering of oxides would not be expected at casting temperatures, and partly because the pocket of gas incorporated in the bifilm would prevent the sides of the defect from coming together.

The presence of these defects has not only the effect of decreasing the mechanical properties of castings, such as their tensile and fatigue properties [2,3], but can also lead to an increase in the scatter of mechanical properties, because the defects formed in the liquid metal would be of variable size, variable orientation, and distributed in a variable way within the fluid flow as the liquid metal filled the mould. These defects tend to be two-dimensional in morphology and can be  $\text{mm}^2$  in size, and may readily be seen on fracture surfaces with the naked eye. These defects are difficult to take into account when designing components containing castings, since unexpectedly low properties may unexpectedly occur, due to the presence of double oxide film defects and their variable nature.

Previous work to reduce the deleterious effects of double oxide films has been chiefly aimed at improving pouring techniques and running system designs in order to reduce or eliminate their formation. Real-time X-ray studies have imaged the behaviour of the liquid metal as it flows within a mould, to determine those features of the running system that might lead to or prevent entrainment of double oxide film defects, and how altering running system design can avoid or reduce them [1,4,5]. Such work has identified good practices such as a minimum ingate velocity of less than  $0.5 \text{ ms}^{-1}$  [4], the use of thin running systems to avoid "rolling back waves" from the end of a runner bar [6], and the use of filters to reduce liquid metal velocity [7]. Tilt pouring has also been shown suggested as a method capable of reducing double oxide film defects [8]. After more than two decades of experimental work, the best solution appears to be countergravity filling, i.e., filling the mould from the bottom in a controlled fashion, for example, by using an electromagnetic pump [9]. While controllable countergravity casting can be applied to low pressure sand and die casting, this requires an investment in equipment, and any advantages associated with countergravity filling may be

lost if double oxide film defects have already been introduced into the liquid metal at some prior stage of the process.

Modelling of oxide film defect formation and their subsequent dispersion during mould filling has also been attempted, [10-13], but such models are usually based on the placement of marker particles, which can poorly represent two-dimensional defects such as double oxide films, with their complex morphology and behaviour, (although an exception is the work by Pita and Felicelli [14]). The lack of a validation method against which to compare simulations of these defects also means that the accuracy of such models cannot be determined.

Some insight into the behaviour of double oxide film defects has been obtained from the experimental work of Griffiths and co-workers [15-17]. Nyahumwa et al. [2] had proposed that the interior atmosphere of a double oxide film defect, presumed to be principally air, would be consumed with time as first oxygen and subsequently nitrogen would react with the surrounding liquid metal. A small residual amount of Ar should eventually be all that remained of the original atmosphere. Raiszadeh and Griffiths [15,16] reported an experiment in which an air bubble was trapped in a SiN rod placed in a furnace containing liquid Al alloy. The air bubble had a diameter of 13.3 mm, and height of 40 mm, and its reduction in volume with time was monitored by real-time X-ray imaging. As the gas in the bubble reacted with the surrounding melt the liquid metal rose up into the blind hole in the SiN rod, preserving the reaction products. The compounds formed during the experiment were examined by Scanning Electron Microscopy (SEM) and Electron Dispersive Spectroscopy (EDS) and found to be alumina and AlN, as expected, (see Figure 2 for an SEM image of AlN). Reaction rates for the formation of alumina and AlN were deduced, and for an estimated double oxide film defect of 5 mm x 5 mm in area, and 40 nm to 40  $\mu$ m in thickness, (derived from Campbell[1]), it was suggested that the internal atmosphere of a double oxide film defect should be consumed in several minutes, or about the period of time in which solidification of a typical Al casting would occur. This suggested that double oxide film defects inside a casting should still be in the process of losing their internal atmosphere during solidification, and therefore would be expected to have a deleterious effect on mechanical properties by increasing their scatter. Alloying additions had different effects on the reaction rates. For example, increasing Mg content decreased the time taken for the air in the bubble to be consumed, but additions of Na and Sr prolonged the time taken for the air in the bubble to be consumed. It was further shown that H dissolved in the surrounding liquid metal would diffuse into the bubble, and by analogy could diffuse into a double oxide film defect, as a casting was undergoing solidification.

A more detailed experiment was reported by El-Sayed et al. [17], in which the composition of the trapped air bubble was determined by mass spectroscopy. Similar behaviour was observed, (reactions that consumed oxygen and nitrogen, and diffusion of H into the air bubble), and the reaction rates determined from this experiment were of order of magnitude agreement with those derived by Raiszadeh and Griffiths [15]. But using a better estimate of double oxide film defect size, obtained from Park[18], (2.2 mm x 2.2 mm x 0.1 mm), led to similar predicted durations of double oxide film defects being deduced.

This experimental work suggested that a possible method to reduce the deleterious effect of double oxide film defects would be to make a chemical addition which would alter the nature of the oxide film on the liquid metal to make it more permeable. A more permeable oxide film could then accelerate the rate of reaction of the gases inside the defect, causing the walls of the defect to come closer together. By reducing the size of the defects their deleterious effects might be minimised, resulting in a reduction in the scatter of mechanical properties, and giving Al castings more reliable and reproducible properties.

Consideration of the Gibbs Free Energy of formation of oxides and of nitrides suggested several elements that might form oxides and nitrides preferentially to alumina or spinel, or AlN[19], (see Tables 1 and 2). It was recognised, of course, that while such additions might alter the composition of the oxides or nitrides formed it might render them less permeable, not more, and might therefore increase the deleterious effect of double oxide film defects.

However, in the course of this work it was discovered that the addition of Mo and W, which were not originally considered to be preferential oxide and nitride-formers, might beneficially affect the tensile properties of Al-Si-Mg alloys. This paper reports the effect of the addition of these two transition metals, Mo and W, to an Al-7Si-0.3Mg alloy, (2L99), and shows their effect on the scatter of measured tensile properties.

## 2. Experimental Procedure.

Mo and W additions were made to an Al-Si-Mg alloy, (2L99), using 2L99-10wt.%Mo and 2L99-10wt.%W masteralloys, respectively. The masteralloys were both made by adding 10 wt.% of the transition metal, (of 99.9 wt.% purity), to 2L99 alloy at 1300°C, followed by holding for 40 minutes.

To investigate the effect of additions of these transition metals the alloys were cast into resin-bonded sand moulds (PEPSET<sup>TM</sup>) to obtain tensile testbars which were used to determine the scatter of tensile properties. For each experiment, approximately 20 kg of 2L99 alloy was melted in an induction furnace and held at  $725^{\circ}\text{C} \pm 5^{\circ}\text{C}$ . Lance degassing with Ar was used to reduce the dissolved H content, followed by casting at a pouring temperature of about  $725^{\circ}\text{C}$  into sand moulds of a design shown in Figure 3. The design of the running system was deliberately intended to produce many double oxide film defects, which were essentially collected in the cylindrical testbars, to allow the examination of the effect of the defects on properties, and determine their composition and morphology on the fracture surfaces.

The sand moulds were made using a resin, and were held in the laboratory for more than one week, in order to reduce the likelihood of H pick-up by the liquid metal due to volatilisation of the resin binder during casting [20]. After casting the moulds were rolled over through  $180^{\circ}$ , to assist feeding during solidification. Each casting produced 10 test-bars.

Initially, several moulds were cast with 2L99 alloy alone, resulting in a total of 77 tensile test-bars. The alloys with the transition metal additions were cast at the same temperature, but with an addition of about 0.4 wt.% Mo or W in each case, using the 10wt.% masteralloys prepared beforehand as described. 30 tensile test bars for each element addition were produced.

To make comparisons of the scatter in mechanical properties, it was necessary to reduce other variations in the alloy compositions that could otherwise contribute to variations in properties. Table 3 shows the actual composition of the cast testbars, (determined using X-Ray Fluorescence, (XRF)), including the amount of Mo and W recovered from the masteralloy addition, and the amount of those elements that might also contribute to the variation in properties of the alloy, such as Mg, Fe, and H, (measured by LECO<sup>TM</sup> [21]). These results confirmed that the experiments had been carried out reproducibly. The transition metal additions resulted in a recovery of 0.39 wt.% Mo and 0.44 wt.% W, the Mg content obtained was consistently between 0.32 and 0.34 wt.%, the Fe content was consistently between 0.07 to 0.12 wt.% and the H content was consistently between 0.13 and 0.18 ppm. Greater variation was observed in the Si content, which lay between 8.1 and 9.9 wt.%.

After casting the testbars were heat-treated to the T6 condition, which required solutionising at  $540^{\circ}\text{C}$  for 12 h, followed by quenching in hot water at  $65^{\circ}\text{C}$ , and then ageing at  $155^{\circ}\text{C}$  for 3.5 h. The testbars were then machined into tensile test specimens of length 100 mm, with a gauge length of 37 mm and a diameter in the gauge length of 6.75 mm.



Following tensile testing the Ultimate Tensile Strength (UTS) and %Elongation results obtained for each alloy were compared by calculating their Weibull Moduli [3], to show the variability of properties obtained with and without the transition metal additions. The fracture surfaces of the test bars associated with the lowest UTS values were also examined, using Scanning Electron Microscopy, (SEM), and Energy Dispersive Spectroscopy, (EDS), using a JOEL 7000 SEM equipped with Oxford INCA software.

### 3. Results.

Figure 4(a-c) shows examples of double oxide film defects on the fracture surfaces of 2L99 alloy, and 2L99+Mo and 2L99+W alloys, respectively, (confirmed by EDS analysis) showing the defects to be  $\text{mm}^2$  in area. The opposing fracture surfaces showed the same defect, symmetrical in appearance as would be expected for a double oxide film defect. Figure 4(d) shows an example of a region of AlN on the fracture surface of an unheat-treated test-bar of the 2L99+Mo alloy.

#### 3.1 Mechanical properties.

Figure 5(a) and 5(b) show examples of stress-strain curves from the different alloys, and how the properties of the 2L99 alloys varied compared to when additions of Mo or W were made, due to their defects. With the three highest %Elongation curves, (Figure 5(a)), the 2L99 alloy, with and without transition metal additions, exhibited similar behaviour, with a UTS of around 300 MPa, and %Elongation of around 3-4%. With the three lowest %Elongation curves, (Figure 5(b)), that of the 2L99 alloy showed potentially the poorest properties, (about 200 MPa and about 0.5% Elongation), but with the transition metal additions, mechanical properties were increased to a UTS of around 250 MPa, and %Elongation of up to around 1%.

Figure 6(a) shows a comparison of the Weibull Moduli for the UTS, for T6 heat-treated Al-7Si-0.3Mg alloy, compared with the Weibull Moduli obtained with additions of about 0.4wt.% Mo and W transition metals. Figure 6(b) shows a similar comparison of the Weibull Moduli for the %Elongation results, and both are summarised in Tables 4(a) and (b). The 2L99 alloy was associated with a Weibull Modulus for the UTS of 16, and a Position Parameter of 277 MPa, (see Figure 6(a) and Table 4(a)). The addition of Mo and W increased the Weibull modulus to 33 and 31, respectively, i.e., by about a factor of two, (111% and 92%, respectively). The addition of Mo and W also increased the Position Parameter by about 10% and 6%, (to 304 and 294 MPa, respectively, (see Table 4(a)).

The 2L99 alloy was associated with a Weibull Modulus for %Elongation of 2.6%, and a Position Parameter of 2.1%, (see Figure 6(b) and Table 4(b)). The addition of Mo increased the Weibull Modulus to 3.1%, (an increase of 20%), and the addition of W increased it to 2.9%, (an increase of 12%). The addition of Mo and W increased the Position Parameter of the %Elongation to about 3.6%, (an increase of about 70%), and to 2.6%, (an increase of 24%), (see Table 4(b)).

In order to compare the Weibull moduli of two data sets, a statistical method was used developed by Tiryakioglu[22]. In this, 2 data sets containing 80 data points and 30 data points, respectively, were generated using a Monte-Carlo simulation, with both sets of data following a Weibull distribution with  $m$  (the Weibull modulus), equal to 1, and  $\sigma_0$  (the Position Parameter), equal to 3. A linear regression method was then used to evaluate the Weibull parameters of the two data sets to give Weibull moduli of  $m_1$  and  $m_2$  respectively. The value of  $m_1/m_2$  was then determined, and the process repeated 10,000 times in order to obtain a clear distribution of results. The 2.5 and 97.5 percentiles of this distribution were

shown to be 0.660 and 1.53, respectively. For the experimental data reported here, the ratio of the two Weibull moduli from the mechanical property tests for any two different sets of testbars was determined, and if this value fell between the range of the 2.5 and 97.5 percentiles obtained as described above, then the two data sets were concluded to be statistically the same. Alternatively, if this value fell outside of the range of the 2.5 and 97.5 percentiles, a statistically significant difference between the data sets was inferred.

Statistical comparisons between the 2L99+Mo or W, and 2L99, have been shown in Table 5. As can be seen, the effect of Mo or W increased the Weibull moduli of the UTS, and this difference was determined to be statistically significant. However, no statistically significant difference between the Weibull moduli of the %Elongation results was found.

### 3.2 Scanning Electron Microscopy

Examples of SEM images of the fracture surfaces of the three different alloys revealed oxides occurring in all cases. Figure 7 shows, in the case of the 2L99 alloy, an oxide usually inferred from EDS analysis to be spinel, ( $\text{MgAl}_2\text{O}_4$ ), which forms in the presence of Mg in Al-Si alloys. Figures 8 and 9 show oxides found on the tensile testbar fracture surfaces of the testbars with Mo and W, respectively, confirmed by EDS. No influence on the composition of the oxide films by the Mo and W additions was apparent; all oxides were determined to be spinel.

In the case of the 2L99 alloy with about 0.4% Mo, while most of the fracture surfaces were associated with oxides, two were found which showed the occurrence of AlN, and which occupied an area of  $5.6 \text{ mm}^2$  and  $0.88 \text{ mm}^2$ , or 16% and 2.5% of the fracture surface, respectively, (see Figures 10(a) and (b)). One of the AlN-containing test bars had the lowest UTS, (255 MPa), of all of the testbars with the Mo addition, (and almost the lowest %Elongation (0.84 %)). The other testbar containing AlN on its fracture surface had a UTS of 274 MPa and %Elongation of 1.58%, approximately similar to the mean values of all of the results. In the case of the castings with an addition of about 0.4% W, no AlN was observed on the fracture surfaces.

Previous experimental work on double oxide film defects in which the fracture surfaces were examined had revealed only aluminium oxides, either alumina in the case of pure Al, spinel in the case of an alloy containing some Mg, or MgO for Al-Mg alloys [23]. The occurrence of AlN on the fracture surfaces of Al alloys has not previously been noted, and its presence on the fracture surface suggested that the interior atmosphere inside this particular double oxide film defect had reached the stage where its oxygen had been largely consumed, and nitrogen remained and was undergoing reaction with the surrounding melt. The EDS analysis suggested that AlN may have formed by nucleation on the spinel oxide film. However, despite being in this stage, as the defect was present on the fracture surface it was still responsible for the failure of the test bar and the double oxide film defect was therefore still operative as a defect that limited mechanical properties.

SEM investigation also revealed the presence of an Al-Si-Mo phase on the fracture surface, (see Figure 11(a), and an Al-W intermetallic, (see Figure 11(b)), suggesting that the presence of intermetallics also had an effect on the mechanical properties of the alloys.

#### 4. Discussion.

The addition of Mo and W increased the Weibull Modulus for both the UTS and %Elongation of the 2L99 (Al-7Si-0.3Mg) alloy, but the mechanisms by which this occurs are not readily identified and could be due to several factors.

Firstly, previous work [2,15,17] was founded on the assumption that it was desirable to accelerate the rate of reaction of the internal atmosphere of double oxide film defects, in an attempt to change their morphology and reduce their deleterious effect on mechanical properties. This suggests that the addition of Mo and W may have resulted in an oxide that offered less resistance to the passage of gas, either by being more permeable, or by having a reduced growth rate and therefore be thinner, or both. This would allow the interior atmosphere of double oxide film defects to react more quickly with the surrounding melt, bringing the walls of the defect closer together, making them less harmful. However, EDS analysis of oxide films on the testbar fracture surfaces did not clearly reveal that Mo or W participated in their formation.

Secondly, the comparison between the 2L99 alloy results, and the Mo- and W-containing 2L99 alloys, was based on 77 testbars of the base alloy, and 30 testbars each in the case of the alloy with transition metal additions whereas the 77 testbars of 2L99 alloy were obtained from 8 moulds which, due to equipment limitations, were cast in 3 different casting experiments, (of 2 moulds, 3 moulds, and another 3 moulds). This in itself would result in more variability than if they were cast all at once, (as were the 30 testbars from the two alloys with transition metal additions).

The role of H dissolved in the melt may also be considered. In an experiment to examine the effect of hydrogen on double oxide film defects it was shown that increased H pick-up by the liquid metal resulted in reduced mechanical properties and an increased scatter of results, (reduced Weibull Modulus)[20]. This was suggested to be due to inflation of double oxide film defects as H from the melt diffused into their interior. More detailed experiments showed the rate of H ingress to be greater in the presence of AlN, compared to a surface coated with oxide[24], probably owing to the greater permeability of an AlN film compared to an oxide film. This suggested that a double oxide film defect in liquid Al can go through an initial stage of oxygen consumption, associated with a low rate of H ingress, followed by a stage of N consumption leading to the formation of permeable AlN, which would be associated with an increased rate of H ingress.

These considerations suggest how the morphology of a double oxide film defect might evolve over time. The initial stage of the lifetime of a double oxide film defect, in which oxygen consumption occurred, might be considered as a period in which the volume of the double oxide film defect would gradually reduce with time, (as a net result of O reaction and H ingress), but this would later be followed by a second stage in which N consumption occurred, during which H could pass into the double oxide film defect more rapidly. In this later stage the volume of the defect would be increased, and therefore in this stage the defect would be most damaging to mechanical properties.

The addition of Mo and W might therefore affect the rate at which dissolved H in the melt can pass into a double oxide film defect. This effect might be brought about by accelerating the growth rate of the oxide film, increasing its thickness, or by generating a less, (not more), permeable oxide film. In either case the rate of H ingress would be reduced, and double oxide film defects would be prevented from becoming enlarged by the ingress of H so quickly. This view suggests that double oxide film defects are not so much damaging to mechanical properties in themselves, but become more so as they are inflated with H during the second, N consumption stage.

Thirdly, the effect of the Mo and W additions may have been to encourage the formation of AlN, (formerly acknowledged to be difficult [25]), possibly by encouraging the formation of  $\text{Mg}_3\text{N}_2$ , previously identified as a desirable precursor.

Finally, the presence of Al-Mo-Si and Al-W intermetallics, (see Figure 11), suggested that Mo and W may act like Fe in Al alloys, forming low melting point intermetallics. However, the Position Parameters for the 2L99 and 2L99+Mo alloys were similar, (with a position parameter of 280 MPa, and %Elongation of 1.3% for the Mo-free 2L99 alloy testbars, and a position parameter of 277 MPa and %Elongation of 1.4% for the Mo-containing alloys), so the nucleation of Mo-rich intermetallics in themselves does not initially appear to be detrimental. But the intermetallics may also nucleate on oxides as Fe-rich intermetallics have been shown to do, and this may lead to removal of oxides by sedimentation of the associated intermetallics[26].

To summarise, the results reported here, particularly the association of AlN on the fracture surfaces with the addition of Mo and an increased Weibull Modulus, suggest that the acceleration of the reaction of the interior atmosphere with the surrounding melt was the most probable explanation for the increased Weibull Modulus, although several mechanisms by which the Weibull Moduli are increased may be acting in combination.

## 5. Conclusions

1. The addition of about 0.4wt.% Mo to an Al-7Si-0.3Mg alloy, doubled the Weibull Modulus of the UTS to 33, and that of the %Elongation to 3%, I.e., by about 20%, measured in the T6 heat-treated state.
2. The addition of about 0.4wt.% W to an Al-7Si-0.3Mg alloy increased the Weibull Modulus of the UTS to about 31, an increase of about 90%, and that of the %Elongation to about 2.9%, an increase of about 13%, measured in the T6 heat-treated state.
3. SEM analysis of double oxide film defects found on the fracture surfaces of the testbars revealed the presence of AlN, whereas previous research had only observed the presence of oxides.
4. The mechanism by which the transition metal additions increase the Weibull Modulus of the 2L99 alloy has not yet been established, but the presence of AlN suggested it was due to the accelerated consumption of the internal atmosphere of double oxide film defects, perhaps reducing their size and therefore their deleterious effects.

## 6. References

1. J. Campbell: 'Complete Casting Handbook', 2nd edn, Chap. 2, 'Entrainment', 19-103; 2011, London, Butterworth-Heinemann.
2. C. Nyahumwa, N. R. Green and J. Campbell: 'The concept of the fatigue potential of cast alloys', *J. Mech. Behaviour Mat.*, 1998, 9, 227-235.
3. N. R. Green and J. Campbell: 'Influence of Oxide Film Filling Defects on the Strength of Al-7Si-Mg Alloy Castings', *AFS Trans.*, 1994, 102, 341-348.
4. J. Runyoro, S. M. A. Boutorabi and J. Campbell: 'Critical Gate Velocities for Film-Forming Casting Alloys: A Basis for Process Specification', *AFS Trans.*, 1992, 37, 225-234.
5. B. Sirrell, M. Holliday and J. Campbell: 'Benchmark Testing the Flow and Solidification Modeling of Al Castings', *proc. 7th. conf. on 'Modelling of casting, welding and advanced solidification processes'*, Warrendale, PA, Paper 56, 915-933.
6. M. R. Jolly, H. S. H. Lo, M. Turan, X. Yang and J. Campbell: 'Development of practical quiescent running systems without foam filters for use in aluminium castings using computer modelling', *proc. 9th Int. Conf. on 'Modeling of Casting, Welding and Advanced Solidification Processes'*, Aachen, Germany, August 2000, *Rwth Aachen University*, Paper 40, 319-325.
7. L. S. Aubrey, J.R. Schmahl and M.A. Cummings: 'Application of Advanced Reticulated Ceramic Foam Filter Technology to Produce Clean Steel Castings', *AFS Trans.*, 1993, 101, 59-69.
8. J. Mi, R. A. Harding and J. Campbell, 'The tilt casting process', *Int. J. Cast Metals Res.*, 2002, 14, 325-334.
9. J. Campbell, Cosworth R&D Ltd.: 'Method and apparatus for melting and casting metal', *US Patent US4967827 A*, 15 August 1989.
10. N. W. Lai, W. D. Griffiths and J. Campbell: 'Modelling of the Potential for Oxide Film Entrainment in Light Metal Alloy Castings', *proc. 10th. Conf. on 'Modelling of Casting, Welding and Advanced Solidification Processes'*, Warrendale, Pennsylvania, May 2003, paper 13, 159-166.
11. X. Yang, X. Huang, X. Dai, J. Campbell and J. Tatler: 'Numerical modelling of entrainment of oxide film defects in filling of aluminium alloy castings', *Int. J. Cast Metals Res.*, 2004, 17, 321-331.
12. C. Reilly, N. R. Green and M. R. Jolly: 'The present state of modeling entrainment defects in the shape casting process', *Appl. Math. Modelling*, 2013, 37, 611-628.
13. C. Reilly, N. R. Green and M. R. Jolly: 'Surface Oxide Film Entrainment Mechanisms in Shape Casting Running Systems', *Met. and Mat. Trans. B*, 2009, 40B, 850-858.
14. C.M. Pita and S.D. Felicelli, 'A fluid-structure interaction method for highly deformable solids', *Computer and Structures*, 2010, 88, 255-262.
15. R. Raeiszadeh and W. D. Griffiths: 'A method to study the history of a double oxide film defect in liquid aluminum alloys', *Met. Mat. Trans. B*, 2006, 37B, 865-871.



16. R. Raiszadeh and W.D. Griffiths: 'A Semi-empirical Mathematical Model to Estimate the Duration of the Atmosphere within a Double Oxide Film Defect in Pure Aluminum Alloy', *Met. Mat. Trans. B*, 2008, 39(2), 298-303.
17. M. A. El-Sayed, H. A. G. Salem, A. Y. Kandeil and W. D. Griffiths: 'Determination of the Lifetime of a Double-Oxide Film in Al Castings', *Met. Mat. Trans. B*, 2014, 45(4), 1398-1406.
18. J. M. Park: 'Behaviours of Bifilms in A356 Alloy during Solidification: Developing Observation Techniques with 3-D Micro X-ray Tomography', MRes, University of Birmingham, Birmingham, UK, 2010, 41-80.
19. R. Raeiszadeh: 'A Method to Study the Behaviour of Double Oxide Film Defects in Aluminium Alloy', PhD Thesis, University of Birmingham, Birmingham, UK, 2005, 81-120.
20. M. A. El-Sayed and W.D. Griffiths: 'Hydrogen, bifilms and mechanical properties of Al castings', *Int. J. Cast Metals Res.*, 2014, 27(5), 282-287.
21. LECO Corporation, 3000 Lakeview Ave., Saint Joseph, MI49085.
22. D. Hudak and M. Tiryakioğlu: 'On comparing the shape parameters of two Weibull distributions', *Mat. Sci. Eng. A*, 2011, 528(27): 8028-8030.
23. S. Impey and D.J. Stephenson: 'A Study of the Effect of Magnesium Additions on The Oxide Growth Morphologies on Liquid Aluminium Alloys', *Proc. 1st. Int. Conf. on 'the microscopy of oxidation'*, Cambridge, UK, 1990: University of Cambridge, 238-244.
24. A. J. Gerrard and W. D. Griffiths, "The formation of Hydrogen related porosity by double oxide film defects in Al alloys", *proc. conf., Shape Casting: 5<sup>th</sup> Int. Symp.*, 2014, TMS 2014, San Diego, CA, 2014, paper 32, 269-276.
25. Q. Zheng and R.G. Reddy: 'Mechanism of in situ formation of AlN in Al melt using nitrogen gas.' *J. Mat. Sci.*, 2004, **39**(1): 141-149.
26. X. Cao and J. Campbell: 'Effect of precipitation and sedimentation of primary  $\alpha$ -Fe phase on liquid metal quality of cast Al-11.1Si-0.4Mg alloy.' *Int. J. Cast Metals Res.*, 2004, 17(1), 496-504.

**List of Table captions.**

Table 1. Gibbs Free Energy of Formation for selected oxides.

Table 2. Gibbs Free Energy of Formation for selected nitrides.

Table 3. Chemical composition of the Al-7Si-0.3Mg alloy castings, with and without the addition of Mo and W.

Table 4(a). Weibull results for UTS values for 2L99 alloy with the addition of transition metals.

Table 4(b). Weibull modulus results for %Elongation values for 2L99 alloy with the addition of transition metals.

Table 5. Statistical comparison of Weibull moduli between 2L99 and 2L99 with Mo or W additions.

### **List of Figure captions.**

Figure 1. Sketch showing the formation of a double oxide film defect, and the encapsulation of a pocket of the local atmosphere during its formation.

Figure 2. SEM micrograph showing an example of AlN, formed in commercial purity Al alloy [15].

Figure 3. Sketch showing the mould design for the production of tensile testbars.

Figure 4. Examples of fracture surfaces containing double oxide film defects from testbars having the lowest tensile properties. (a). L99 alloy, having UTS=204 MPa and %Elongation 0.66%. (b). L99+Mo alloy, having UTS=255 MPa and %Elongation 0.84%. (c). L99+W alloy, having UTS=262 MPa and %Elongation 0.89. (d). Example of a fracture surface exhibiting AlN, (UTS=247 MPa, %Elongation=0.71%).

Figure 5(a). Examples of strain-stress curve from testbars with the highest %Elongation values from the three different alloys. (b). Examples of strain-stress curve from testbars with the lowest %Elongation values from the three different alloys.

Figure 6(a). The Weibull moduli for UTS for transition metals added to 2L99 alloy.

Figure 6(b). The Weibull moduli for %Elongation for transition metals added to 2L99 alloy.

Figure 7. SEM image, and associated EDS, of an oxide film defect on the fracture surface of a 2L99 alloy testbar, indicating the presence of spinel.

Figure 8. SEM image, and associated EDS, of an oxide film defect on the fracture surface of a 2L99+Mo alloy testbar, indicating the presence of spinel. (The peak for Mo occurs at 2.3 keV).

Figure 9. SEM image, and associated EDS, of an oxide film defect on the fracture surface of a 2L99+W alloy testbar, indicating the presence of spinel. (The peak for W occurs at 8.4 keV).

Figure 10(a). SEM image of AlN found on the fracture surface of a 2L99+Mo testbar, together with associated EDS.

Figure 10(b). A higher magnification image of the AlN found on the fracture surface of a 2L99+Mo testbar, with associated EDS analysis.

Figure 11(a). SEM image and EDS analysis of an intermetallic phase found on the fracture surface of a tensile test bar, alloy 2L99+Mo.

Figure 11(b). SEM image and EDS analysis of an intermetallic phase found on the fracture surface of a tensile test bar, alloy 2L99+W.

## TABLES

Element	Oxide	Gibbs Free Energy of Formation (kJ / molO <sub>2</sub> )
Al	Al <sub>2</sub> O <sub>3</sub>	-907.55
Zr	ZrO <sub>2</sub>	-909.94
Li	Li <sub>2</sub> O	-932.81
Al+Mg	MgAl <sub>2</sub> O <sub>4</sub>	-939.97
Hf	HfO <sub>2</sub>	-961.14
Sr	SrO	-982.46
Mg	MgO	-985.72
La	La <sub>2</sub> O <sub>3</sub>	-1005.11
Ce	Ce <sub>2</sub> O <sub>3</sub>	-1008.77
Be	BeO	-1020.15
Ca	CaO	-1062.17
Sc	Sc <sub>2</sub> O <sub>3</sub>	-1075.71
Y	Y <sub>2</sub> O <sub>3</sub>	-1076.34

Table 1. Gibbs Free Energy of Formation for selected oxides.

Element	Nitride	Gibbs Free Energy of Formation (kJ / molN <sub>2</sub> )
Al	AlN	-423.6
Sc	ScN	-427.93
Ti	TiN	-486.14
Zr	ZrN	-543.53
Hf	HfN	-567.49

Table 2. Gibbs Free Energy of Formation for selected nitrides.

Composition (wt.%)	Al	Si	Mg	Fe	Ti	Mn	Mo	W	H (ppm)	Number of test- bars
2L99 (mean of 3 casting experiments).	Bal.	8.74	0.32	0.09	0.13	-	-	-	0.18	77
2L99 + Mo	Bal.	8.12%	0.32	0.12	0.10	-	0.39	-	0.16	30
2L99 + W	Bal.	9.93%	0.33	0.09	0.14	-	-	0.44	0.13	30

Table 3. Chemical composition of the Al-7Si-0.3Mg alloy castings, with and without the addition of Mo and W.

	2L99	2L99+Mo	2L99+W
Weibull Modulus for UTS (MPa)	16.1	33.9	30.9
Position Parameter for UTS (MPa)	277	304	294
R <sup>2</sup> value	0.98	0.97	0.98

Table 4(a). Weibull results for UTS values for 2L99 alloy with the addition of transition metals.

	2L99	2L99+Mo	2L99+W
Weibull Modulus for Elongation (%)	2.55	3.05	2.89
Position Parameter for Elongation (%)	2.13	3.58	2.55
R <sup>2</sup> value	0.98	0.96	0.94

Table 4(b). Weibull modulus results for %Elongation values for 2L99 alloy with the addition of transition metals.

Comparison	m <sub>1</sub> /m <sub>2</sub> ratio for UTS	Significant difference between two data sets?	m <sub>1</sub> /m <sub>2</sub> ratio for %Elongation	Significant difference between two data sets?
2L99 and 2L99+Mo	0.49	Yes	0.74	No
2L99 and 2L99+W	0.52	Yes	0.88	No

Table 5. Statistical comparison of Weibull moduli between 2L99 and 2L99 with Mo or W additions.

## FIGURES

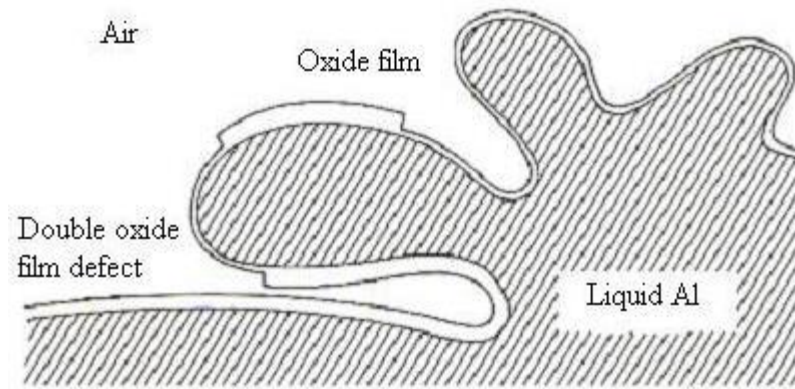


Figure 1. Sketch showing the formation of a double oxide film defect, and the encapsulation of a pocket of the local atmosphere during its formation.

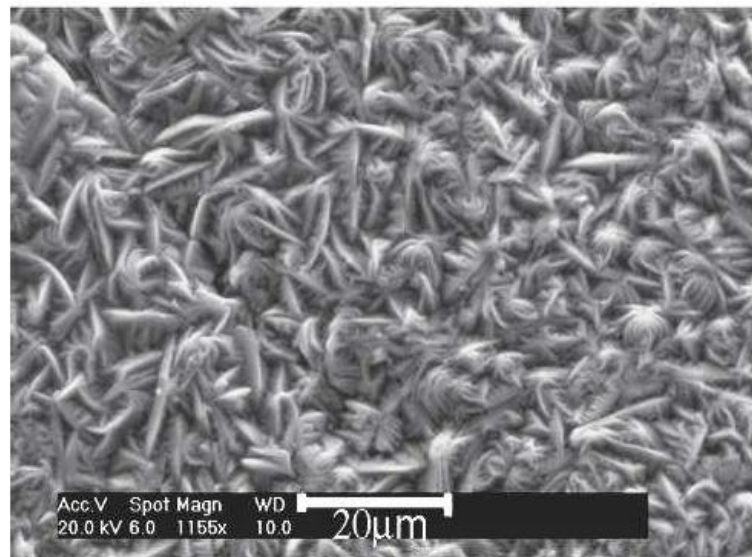


Figure 2. SEM micrograph showing an example of AlN, formed in commercial purity Al alloy [15].

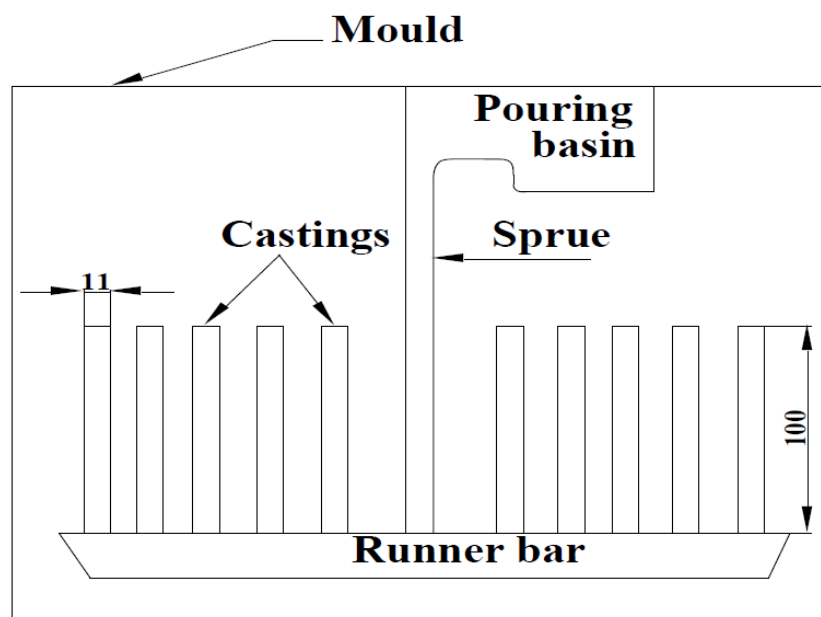
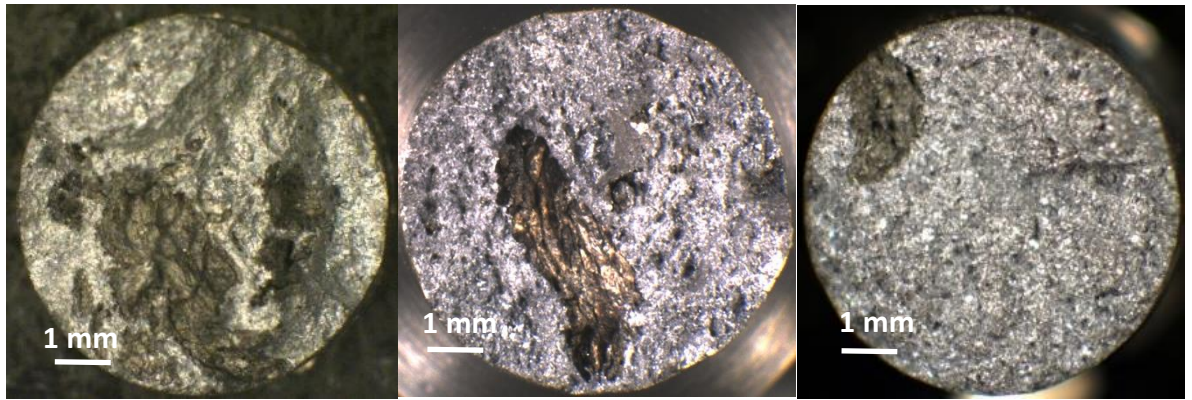


Figure 3. Sketch showing the mould design for the production of tensile testbars.



(a).

(b).

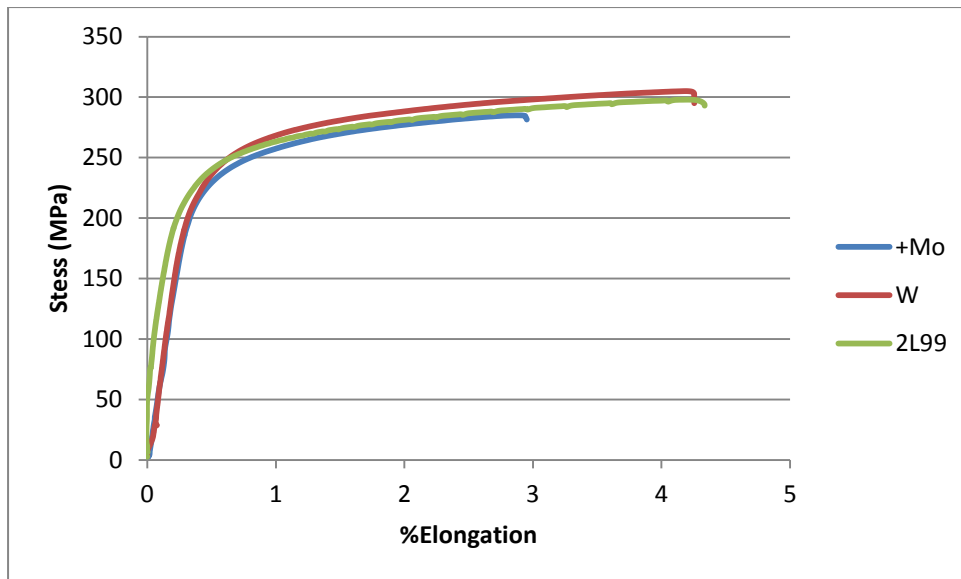
(c).



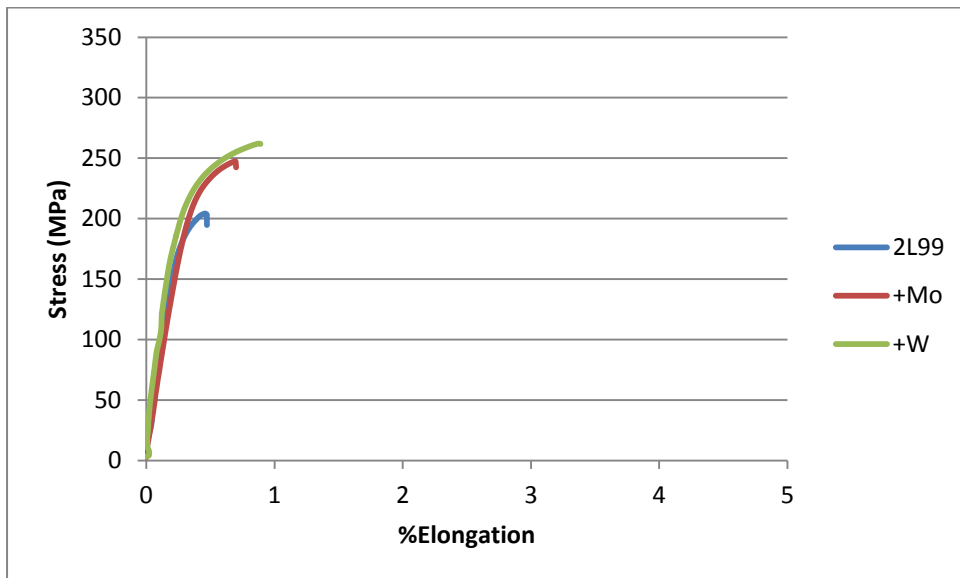
(d).

Figure 4. Examples of fracture surfaces containing double oxide film defects from estbars having the lowest tensile properties. (a). L99 alloy, having UTS=204 MPa and %Elongation 0.66%. (b). L99+Mo alloy, having UTS=255 MPa and %Elongation 0.84%. (c). L99+W alloy, having UTS=262 MPa and %Elongation 0.89. (d). Example of a fracture surface exhibiting AlN, (UTS=247 MPa, %Elongation=0.71%).





(a).



(b).

Figure 5(a). Examples of strain-stress curve from testbars with the highest %Elongation values from the three different alloys. (b). Examples of strain-stress curve from testbars with the lowest %Elongation values from the three different alloys.

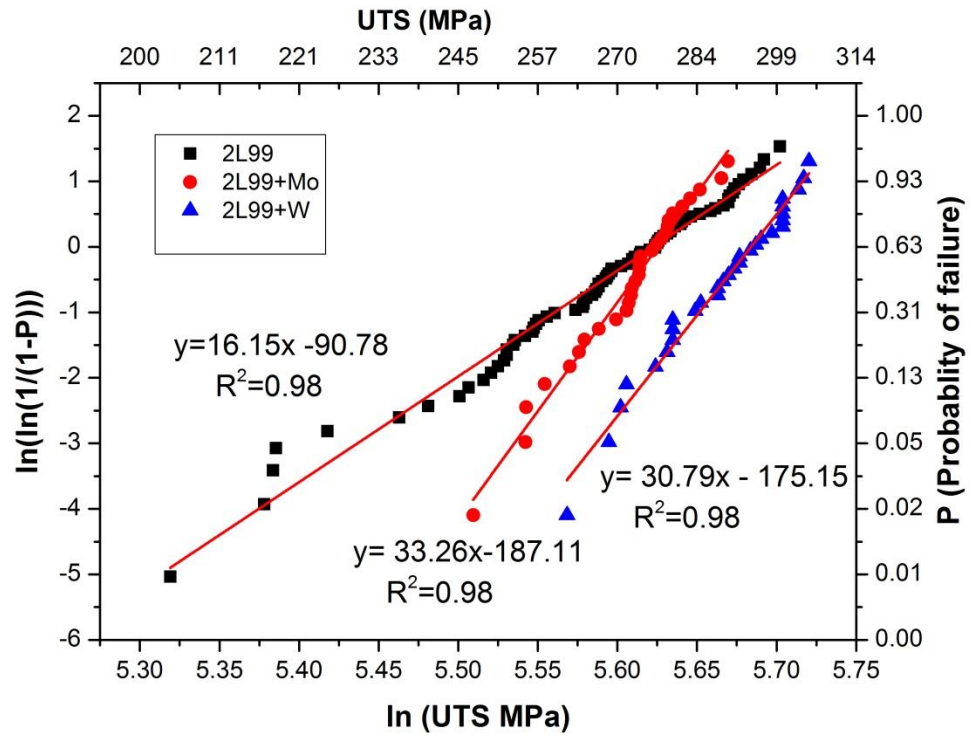


Figure 6(a). The Weibull moduli for UTS for transition metals added to 2L99 alloy.

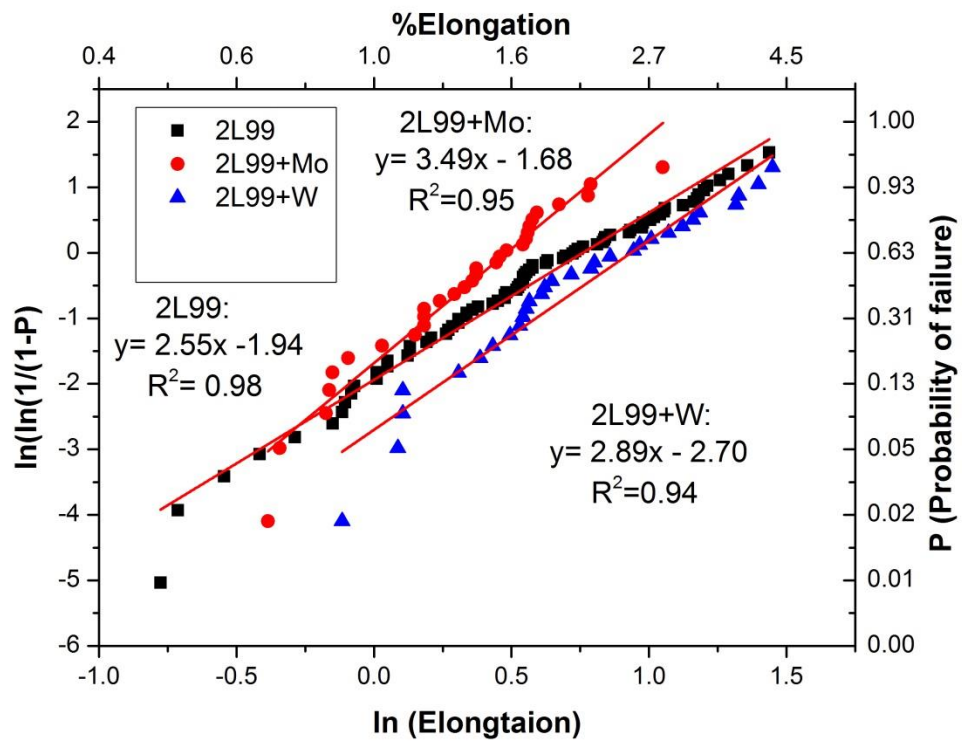


Figure 6(b). The Weibull moduli for %Elongation for transition metals added to 2L99 alloy.

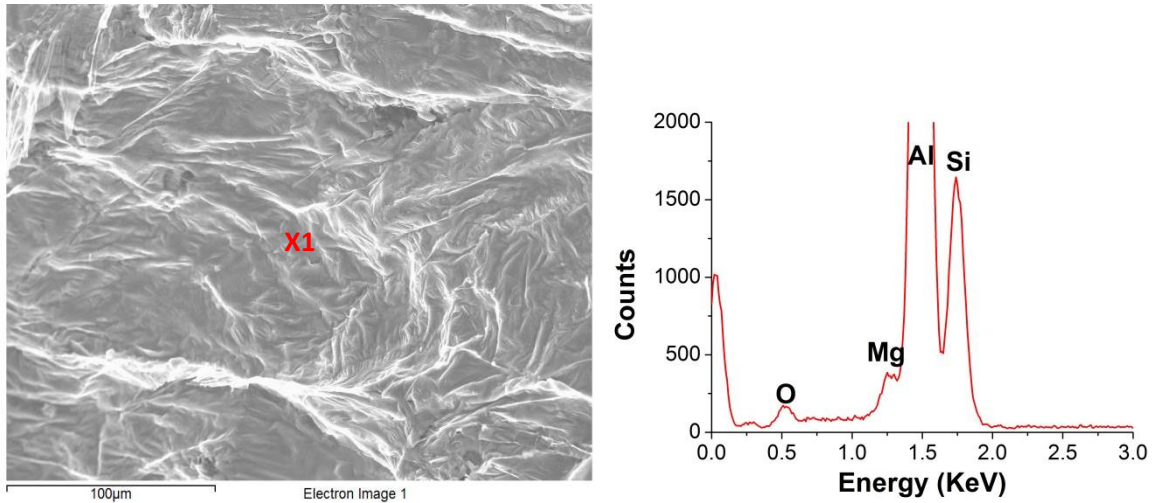


Figure 7. SEM image, and associated EDS, of an oxide film defect on the fracture surface of a 2L99 alloy testbar, indicating the presence of spinel.

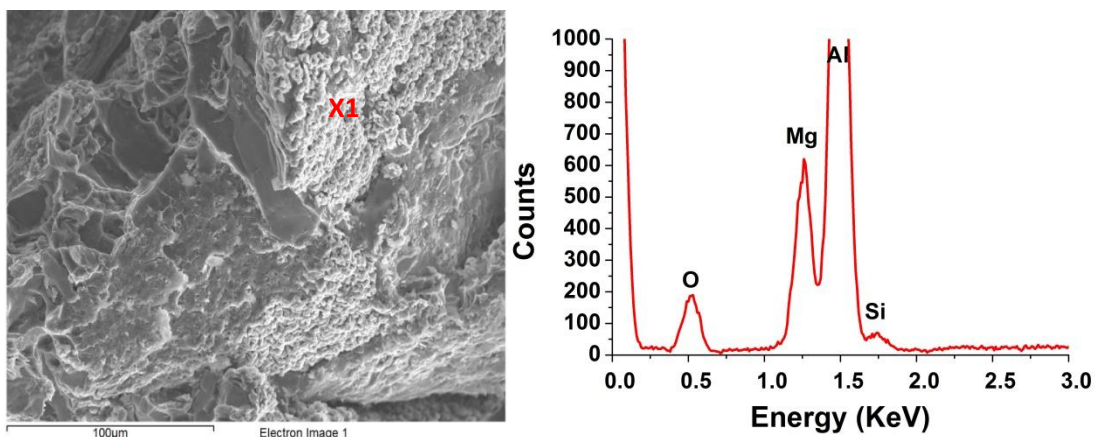


Figure 8. SEM image, and associated EDS, of an oxide film defect on the fracture surface of a 2L99+Mo alloy testbar, indicating the presence of spinel. (The peak for Mo occurs at 2.3 keV).

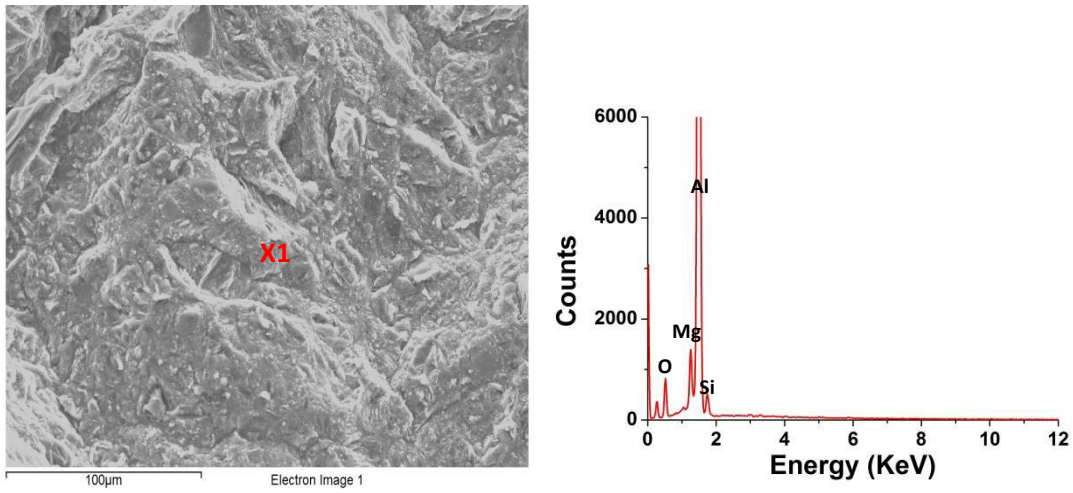


Figure 9. SEM image, and associated EDS, of an oxide film defect on the fracture surface of a 2L99+W alloy testbar, indicating the presence of spinel. (The peak for W occurs at 8.4 keV).

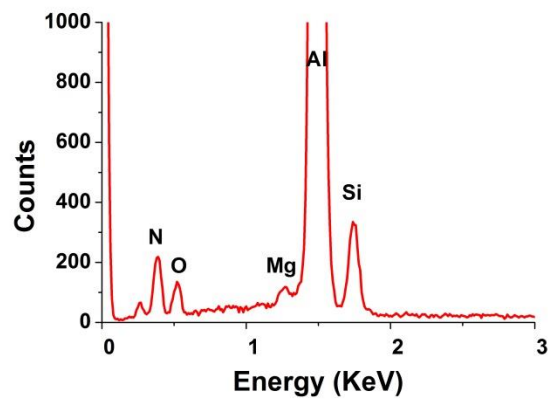
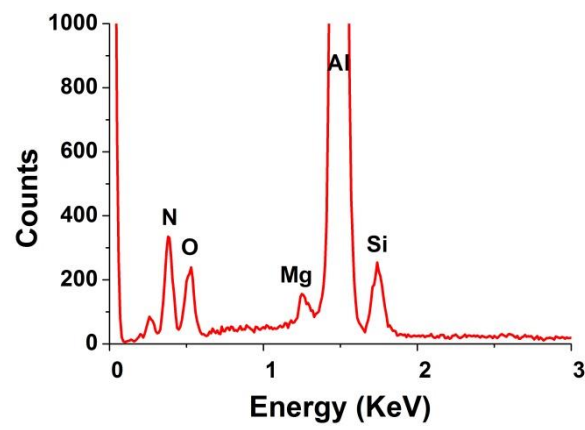
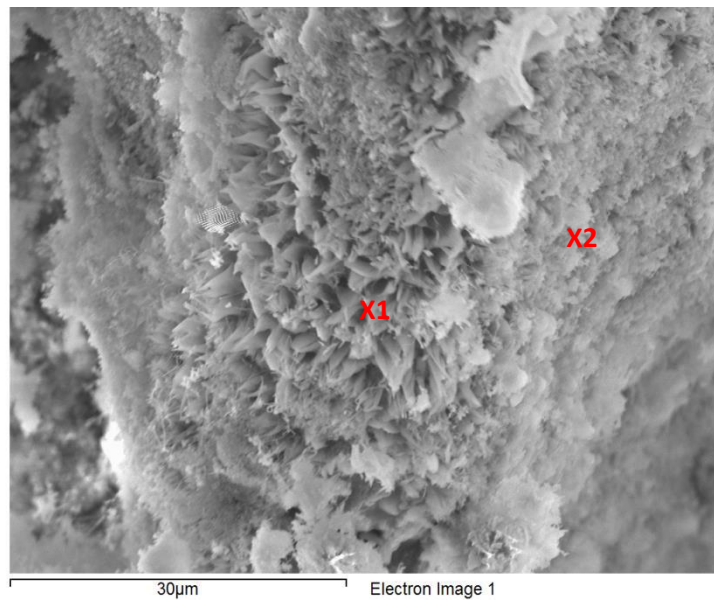


Figure 10(a). SEM image of AlN found on the fracture surface of a 2L99+Mo testbar, together with associated EDS.

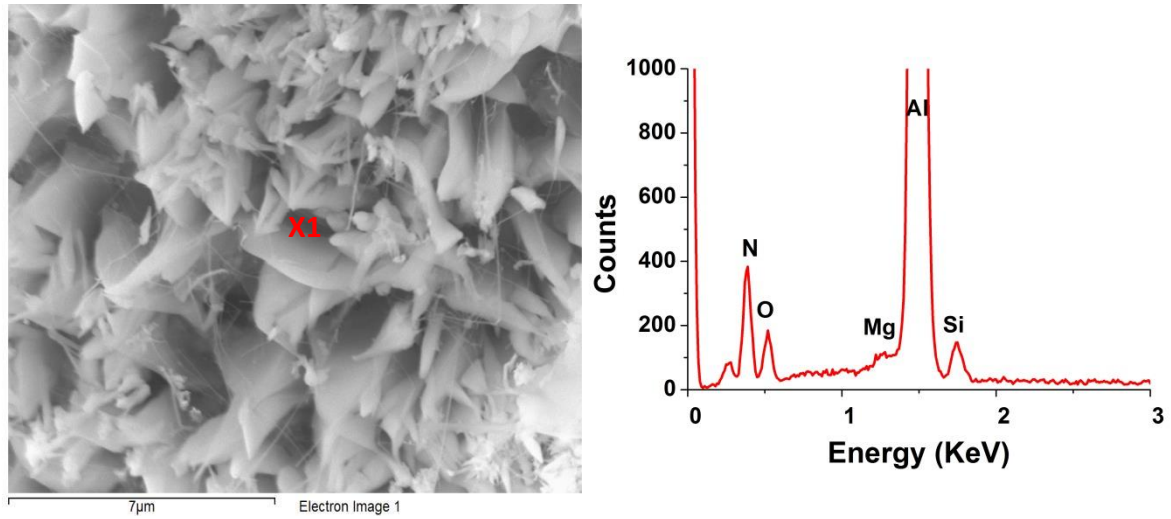


Figure 10(b). A higher magnification image of the AlN found on the fracture surface of a 2L99+Mo testbar, with associated EDS analysis.



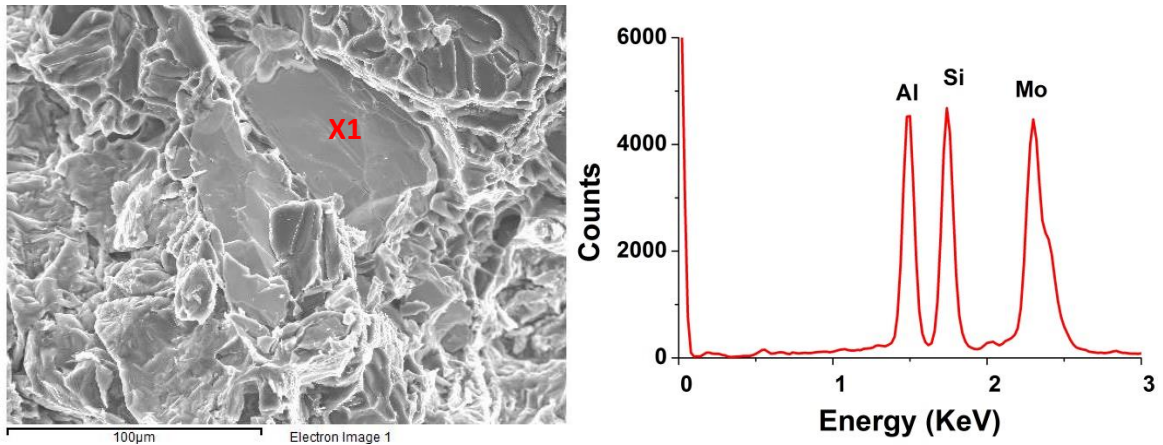


Figure 11(a). SEM image and EDS analysis of an intermetallic phase found on the fracture surface of a tensile test bar, alloy 2L99+Mo.

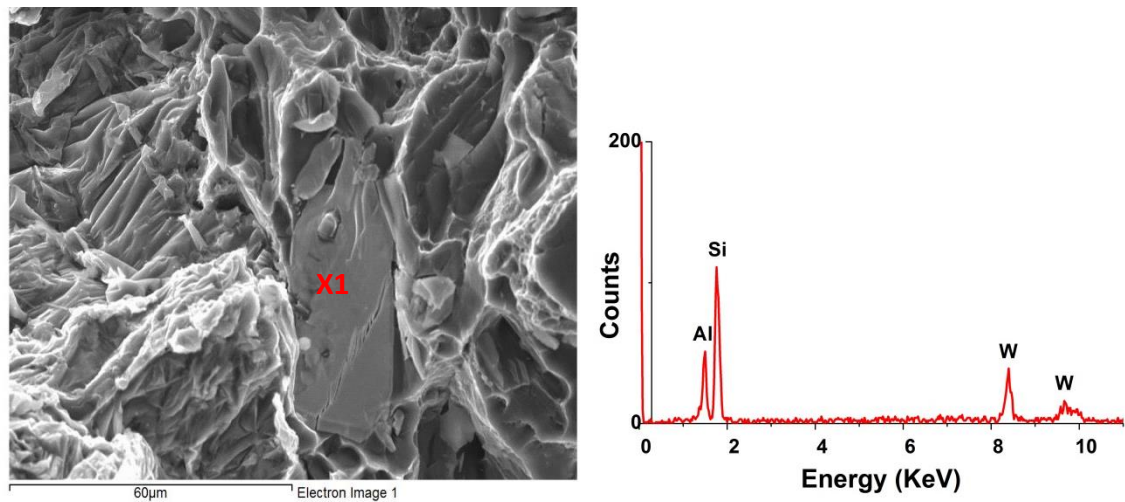


Figure 11(b). SEM image and EDS analysis of an intermetallic phase found on the fracture surface of a tensile test bar, alloy 2L99+W.